Chiral Discrimination of a Gemini-Type Surfactant with Rigid Spacer at the Air−Water Interface

ARTICLE *in* THE JOURNAL OF PHYSICAL CHEMISTRY B · NOVEMBER 2007

Impact Factor: 3.3 · DOI: 10.1021/jp074279i · Source: PubMed

2 AUTHORS, INCLUDING:

vijai shankar Balachandran
Reliance Industries Limited
13 PUBLICATIONS **209** CITATIONS

Chiral Discrimination of a Gemini-Type Surfactant with Rigid Spacer at the Air−Water Interface

B. Vijai Shankar and Archita Patnaik*

Department of Chemistry, Indian Institute of Technology Madras, Chennai 600 036, India

Received: June 3, 2007; In Final Form: July 7, 2007

Spontaneous separation of chiral phases was observed in the monolayers of a racemate of gemini-type twin-tailed, twin-chiral amphiphiles, (2*R*,3*R*)-(+)-bis(decyloxy)succinic acid and (2*S*,3*S*)-(−)-bis(decyloxy)succinic acid. The pressure−area isotherms of the interfacial monolayers formed at the liquid−air interface, and the 2D lattice structures studied through surface probe measurements revealed that the racemate exhibits a homochiral discrimination of the enantiomers in two dimensions. An enantiomeric excess (*e*,*e*) of 20% was sufficient to break the chiral symmetry at the air−water interface for a homochiral interaction. Langmuir monolayers on $ZnCl_2$ and $CaCl_2$ subphases manifested chiral discrimination with Zn^{2+} evidencing homochiral interaction with a chelate-type complex, whereas Ca^{2+} resulted in a heterochiral interaction forming an ionic-type complex. For the chiral asymmetric units, oblique and rectangular unit cells of the racemic monolayer had exclusive requirements of homo- and heterochiral recognitions for Zn^{2+} and Ca^{2+} ions, respectively. Monolayers transferred from the condensed phase at 25 mN/m onto hydrophilic Si(100) and quartz substrates revealed the formation of bilayers through transfer-induced monolayer buckling. The emergence of homochiral discrimination was explained using the effective-pair-potential (EPP) approach.

Introduction

Nature adopts a "code of conduct" or systemic discipline for the precise execution of several vital biochemical processes. It provides subtle clues to decipher myriad scientific challenges that are apparently mysterious. Chirality is one such excellent property with which supramolecular chemistry in nature is performed in a controlled manner to realize functional structures that are highly selective and specific. The phenomenon of chirality could therefore be observed from microscopic to mesoscopic biological systems.[1] Chiral transcription of individual chirality of a molecular system to a two-dimensional (2D) supramolecular assembly has therefore invited increasing attention in the recent past.[2−4] Chiral expression at surfaces or simply 2D chirality is the cynosure, as it could be exploited for its closer similarity to a real model system of a stereospecific membrane as well as its potential over a spectrum of disciplines from organic synthesis to materials chemistry.[5]

The objective of exploring chirality in two dimensions could be a concise doublet: (1) biomembranes are chiral, and (2) chiral molecules have a complicated crystalline arrangement in bulk solids. It is simpler to study the chiral forces in two dimensions, as the degrees of freedom in the other two planes are restricted. Two-dimensional chiral films[6] achieved through different noncovalent interactions help in understanding the phenomena at the molecular level. Monolayers at the air−water interface are an ideal example of physical systems where chirality is studied in two dimensions. Here, surface pressure is a thermodynamic variable and hence permits systematic study of chiral forces in a membrane. With the availability of characterizing systems at the molecular level either in situ or off situ, such as surface probe measurements (SPM),[7] grazing incidence X-ray diffraction, (GIXRD),[8] and polarization-modulated infrared reflection absorption spectroscopy (PM-IRRAS),[9] Langmuir monolayers and Langmuir−Blodgett films receive renewed attention. Chiral discrimination or chiral symmetry breaking in monolayers at the air−water interface has been focused with greater interest owing to its direct consequence of many enzymatic processes at membrane surfaces.[10]

The phenomenon of chiral discrimination arises from a nonequivalence of the interaction potentials between molecules of identical chirality against that of opposite chirality. If the interaction is more favored between either *R*−*R* or *S*−*S* enantiomers, it is termed as a homochiral interaction, while a more favorable interaction between *R*−*S* enantiomers is termed as a heterochiral interaction. This phenomenon is manifested in the 2D arrangement of molecules in the condensed phase, where differences arise due to the disparities among the thermodynamic and macroscopic properties of the monolayer.

Thus, long-chain amino acid derivatives,[11] hydroxy-substituted fatty acids,[12] binols,[13] and gemini surfactants[14] have been studied at the air−water interface. The term "gemini" refers to a dimeric surfactant with its head groups connected by either a rigid or flexible spacer. They offer expanded structural diversity, as the length of hydrophobic chains, headgroups, and counterions can each be varied in a search for enhanced performance.[15] Therefore, gemini surfactants are potential candidates for fundamental studies of organized molecular assemblies in two dimensions. While the properties of gemini surfactants in aqueous solution have been the main focus of investigation, recent studies have focused on monolayers of gemini surfactants at the air−water interface.[16] Liu et al. reported the 2D crystallization of a gemini surfactant with a rigid phenyl methylene spacer.[17] As most of the gemini surfactants are synthetic, biocompatible, or biodegradability, ensure their efficient utilization in eco-friendly processes. Tartaric acid-based gemini surfactants[18] are ideal in such a purview. Singh et al. explored the thermotropic phase transition behavior of alkoxy-

* Corresponding author. Tel: +91-44-22574217. Fax: 91-44-22574202. E-mail: archita59@yahoo.com.

10.1021/jp074279i CCC: $37.00
Published on Web 09/11/2007

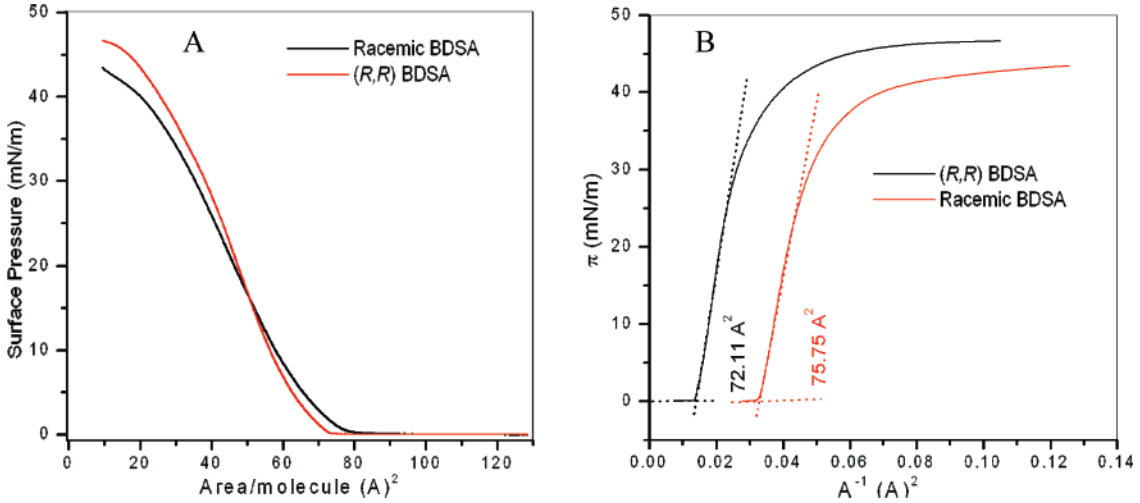

Figure 1. (A) Pressure−area ($\pi-A$) isotherms of enantiomeric and racemic BDSA on Millipore water at 25 °C. (B) $\pi-A^{-1}$ plots for enantiomeric and racemic BDSA. The racemic profile in ($\pi-A^{-1}$) is shifted +0.02 area units for clarity.

CHART 1: (a) Molecular Structure of (*R,R*) BDSA; (b) Geometry-Optimized (B3LYP/6-31G) Structure of (*R,R*) BDSA in Its Constrained Form with the Connolly Surface Showing the Area per Molecule 71.86 Å²

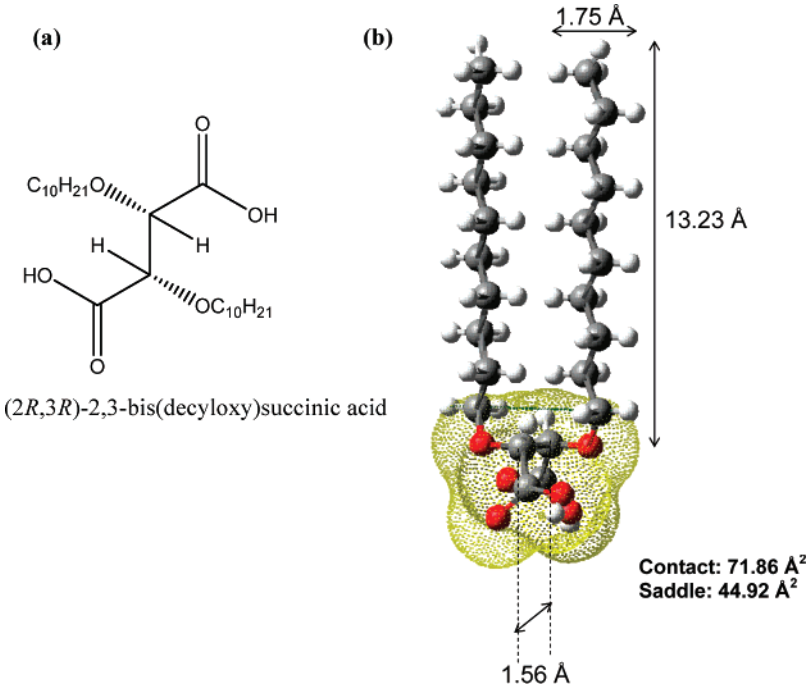

lated tartaric acid derivatives with complementary bases.[19] Fouqey et al. reported the self-assembling behavior of the same in bulk organic media.[20] Recently, Aratani et al. reported the bulk-phase rheological and phase behavior of a dimeric gemini-type surfactant with a rigid spacer.[21] In our earlier work, we reported the self-assembling properties of enantiomerically pure sodium bis(decyloxy)succinates in aqueous solution to form pH-dependent myelin figures and spontaneous vesicles in aqueous solution.[22] The molecule was unique in its behavior with two vicinal carboxyl head groups attached directly to the chiral centers. Chiral transcription from point chirality to supramolecular chirality was observed in forming stimuli-responsive hydrogels from tartaric acid-based surfactants.[23] However, there are no reports so far on the 2D behavior of chiral gemini surfactants where the head groups are directly linked without any bridge between them.

In the present work we report the chiral discrimination behavior of 2,3-bis(decyloxy)succinic acid (BDSA) at the air−water interface and explore its phase behavior, metal-ion-assisted chiral discrimination, and self-assembling behavior in two dimensions.

Experimental

Synthesis. (2*R*,3*R*)-(+)-bis(decyloxy)succinic acid, (2*S*,3*S*)-(−)-bis(decyloxy)succinic acid, and (±)-bis(decyloxy)succinic acid (collectively termed as BDSA) were synthesized according to the reported procedure.[22,24]

Pressure−Area Experiments. The monolayers were spread from chloroform (Uvasol, Merck) solutions on the surface of ultrapure water (Millipore-Academic) of resistivity 18.2 MΩ cm and pH ∼ 5.55−5.65 (normal) in equilibrium with atmospheric CO_2. The temperature of the subphase was maintained at a desired temperature using the Julabo F-36 temperature controller with an accuracy of ±0.1 °C. The pH of the subphase was altered by adding sulfuric acid (for acidic pH) or $NaHCO_3$ (for basic pH). Surface pressure−molecular area ($\pi-A$) iso-

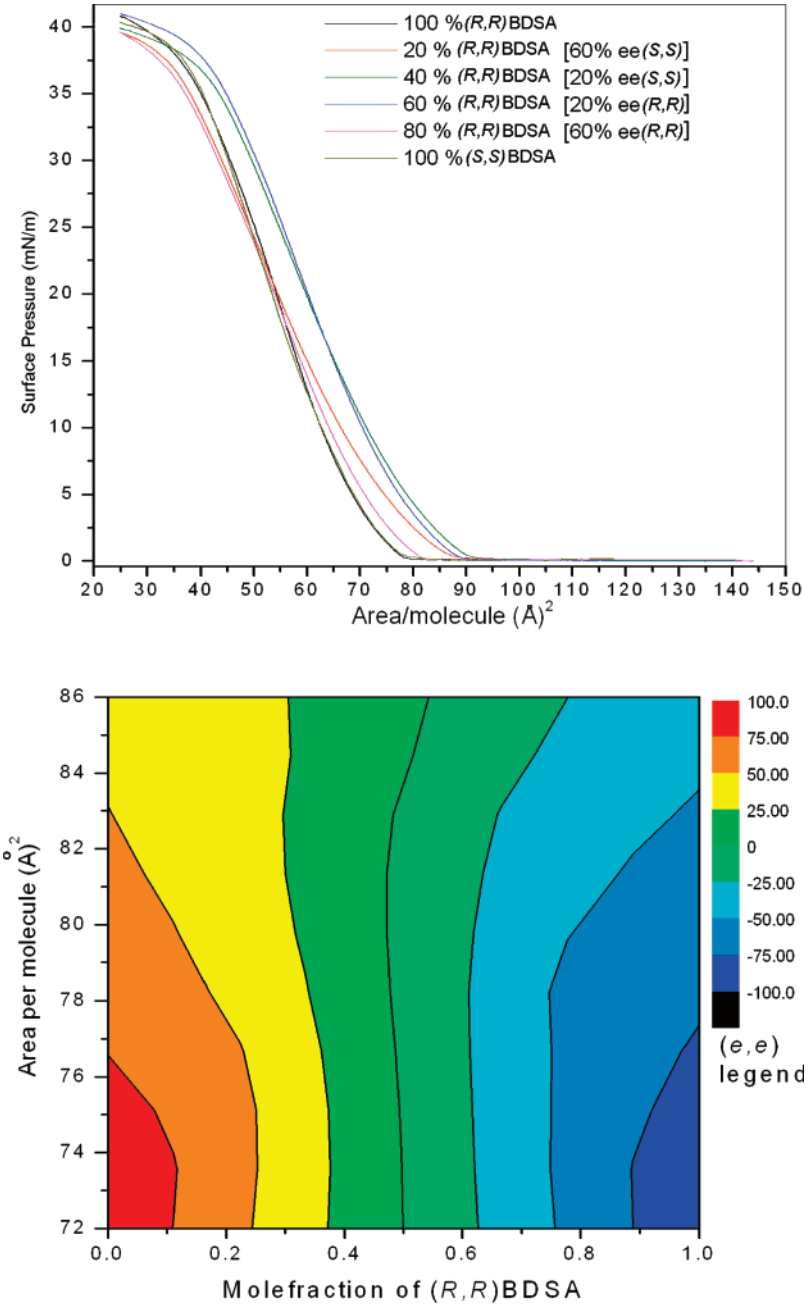

Figure 2. Pressure−area (π−A) isotherms of BDSA with different enantiomeric excesses at 25 °C. At the bottom is shown the contour representation of (*e*,*e*) against the area per molecule for different mole fractions of (*R*,*R*) BDSA in an (*S*,*S*) BDSA monolayer. The negative value of the (*e*,*e*) legend refers to the (*S*,*S*) enantiomer.

therms were obtained on a computer-controlled double-barrier Langmuir trough, KSV 5000 (Finland). For a fresh run, the trough was cleaned thoroughly with HPLC grade chloroform, followed by methanol (extrapure AR, SRL fine chemicals, India), and finally rinsed with Millipore water.

For isotherm measurements, 100 μL of 1 mM solution was spread using a gas tight Hamilton syringe and the surface pressure was measured by the Wilhelmy method with a platinum sensor of accuracy 0.1 mN/m. A delay of 30 min was allowed for the solvent to evaporate before acquiring the isotherms. The Langmuir films were compressed at an optimized speed of 10 mm/min. The Langmuir−Blodgett films were prepared by transferring the monolayers at a desired pressure by the vertical dipping method on hydrophilized Si(100) and quartz plates. Hydrophilization was done by etching the substrates with hot piranha solution (1:1 con. H_2SO_4/H_2O_2) at 70 °C followed by rinsing with Millipore water. The substrates were etched fresh prior to the use for every transfer and stored in Millipore water.

Microscopy. Optical microscopy was performed with an Olympus BX-60 microscope fitted with a color CCD camera (Evaluation series-Media Cybernetics). Transmission electron microscopy was done with a Phillips CM-50, and HRTEM was done on a JEOL 3010 instrument. Atomic force microscopy was performed on a Nanoscope IV (Digital Instruments) in tapping mode with a silicon cantilever.

Results and Discussion

Monolayer Behavior of BDSA at the Air−Water Interface. The molecular structure of (*R*,*R*) BDSA is shown in Chart 1a. The structure was geometry optimized with the alkyl chains constrained to an upright orientation using the *Gaussian 03* package at the B3LYP/6-31G level of theory, as shown in Chart

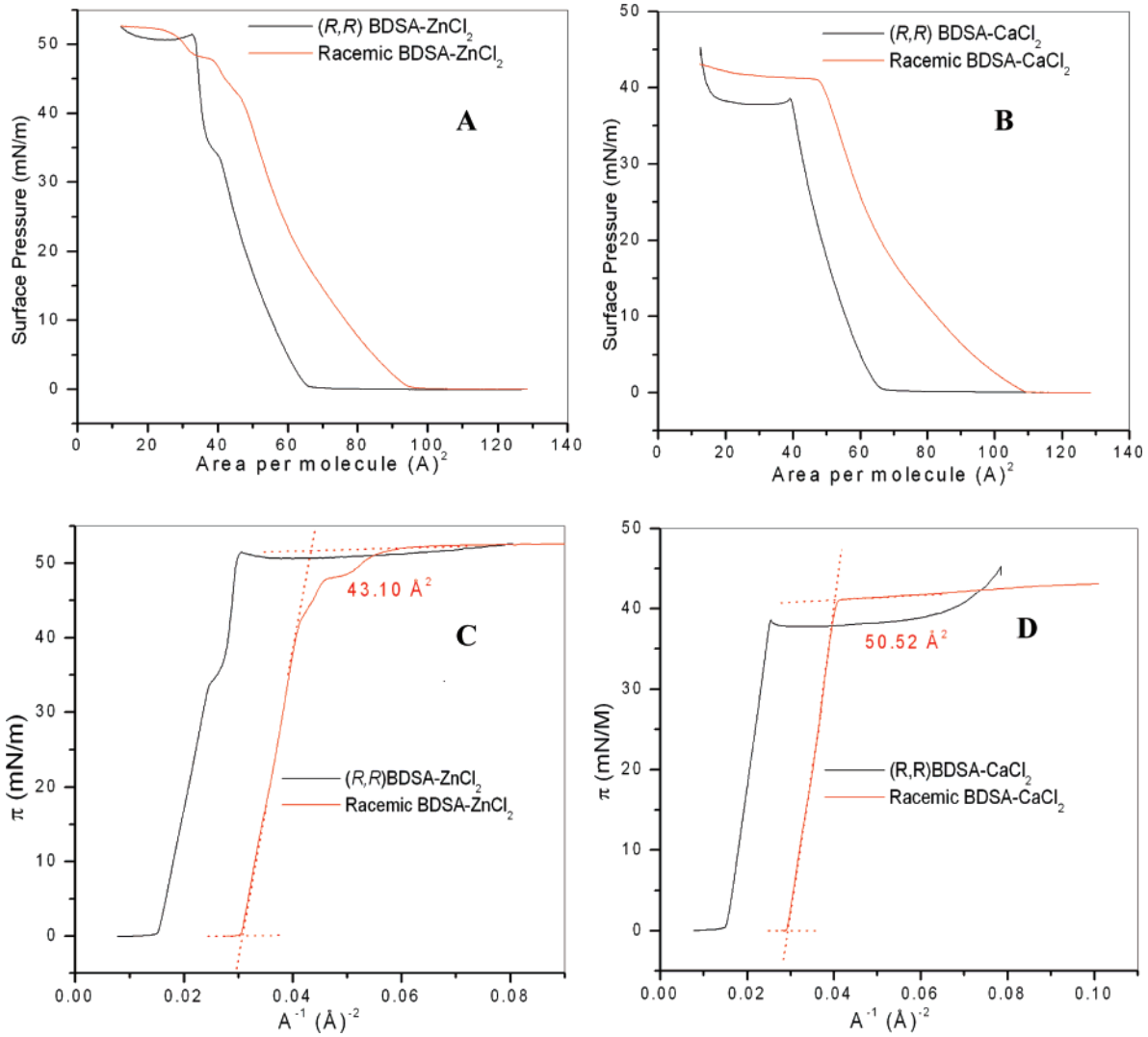

Figure 3. Pressure−area ($\pi-A$) isotherms of BDSA at 25 °C on subphases containing (A) 1 mM $ZnCl_2$ and (B) 1 mM $CaCl_2$; (C) and (D) are the corresponding ($\pi-A^{-1}$) plots. The racemic isotherms in ($\pi-A^{-1}$) plots are shifted +0.02 area units for clarity.

1b. The pressure−area ($\pi-A$) isotherms of enantiomeric BDSA on Millipore water at 25 °C are shown in Figure 1A. The isotherms show an expanded behavior evidencing the following sequence: gas (G) → liquid condensed (LC) → solid phase (S). The area per molecule by extrapolating the condensed region to zero pressure was found to be ∼70 Å.^{2} Connolly surface calculations of the optimized structure revealed the head group area to be 71.86 Å^2, suggesting an upright orientation at the air−water interface. The $\pi-A$ isotherms of a racemic BDSA mixture showed a slight increase in the area per molecule with a small decrease in the collapse pressure when compared to the pure enantiomers.

A detailed analysis of the pressure−area isotherms was made using a $\pi-A^{-1}$ plot. This follows from the methodology deduced by Valkova et al. from the 2D equation of state for monolayer films.[25] The $\pi-A^{-1}$ plots for the compression of the enantiomerically pure and racemic mixtures are shown in Figure 1B. The area per molecule was clearly identified to be 72.11 Å^2 for the enantiomers and 75.75 Å^2 for the racemic mixtures. Enantiomeric monolayers have been reported to exhibit a more condensed isotherm than the racemic one for a homochiral interaction.[26] The present observation thus suggested a homochiral interaction to persist with the racemic monolayers at the air−water interface. The self-assembling behavior was predicted by calculating the critical packing parameter p given by $p = V/(a_s l_c)$, where V is the volume of the hydrocarbon chain, l_c is the critical chain length assumed to be equal to the fully extended chain length, and a_s is the head group area.[27] The value of $p = 1$ suggested the formation of planar bilayers at the respective surface molecular density achieved upon compression.

Control of Enantiomeric Excess (*e*,*e*) on Chiral Symmetry Breaking. The $\pi-A$ experiments were performed with different enantiomeric excesses as shown in Figure 2. The isotherm for the (*R*,*R*) enantiomer with 20% (*e*,*e*) of (*S*,*S*) shows an increased area per molecule as 84.78 Å^2, suggesting the presence of 20% (*S*,*S*) excess to be sufficient enough to break the chiral symmetry in the monolayer and propagate the homochiral discrimination in two dimensions. Ernst et al. have observed the sergeant−soldier effect of coadsorbed (*R*,*R*) tartaric acid on the adsorption of succinic acid monolayers on Cu(110). The studies revealed that a 2% doping of the former was sufficient to generate global homochirality for breaking the reflection symmetry.[28] Such a phenomenon is exciting from the application view point to induce chiral discrimination in a racemic monolayer by "seeding" with an enantiomeric excess.[29]

Metal-Ion-Directed Chiral Discrimination in the Racemic BDSA LB Films. It is well-established that the presence of bivalent cations in the subphase assists cation-dependent condensation of fatty acid monolayers at the air−water interface.[30] The isotherms were acquired on subphases containing 1

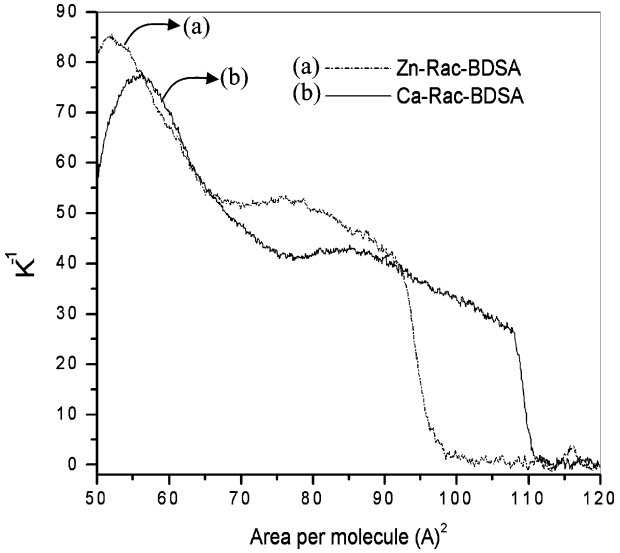

Figure 4. Isothermal compressibility plots of racemic BDSA on subphases containing Zn^{2+} and Ca^{2+} ions in the subphase.

mM $ZnCl_2$ and 1 mM $CaCl_2$ and are shown in Figure 3, parts A and B. The isotherms evidenced distinct differences in their features, characteristic of the metal ions. The $\pi-A^{-1}$ isotherms of the racemic monolayers, vide Figure 3, parts C and D, revealed an area per molecule of 90.10 and 108.69 Å^2 for Zn^{2+} and Ca^{2+}, respectively. Huehnerfuss et al. reported the effect of cations on the order of the saturated fatty acid monolayers at the air−water interface.[31] Sakai et al. studied the modes of binding of Zn^{2+} to 12-hydroxy stearic acid through external reflection IRRAS, evidencing the chelate-type binding of Zn^{2+} to the carboxyl groups.[32] Since in BDSA the two carboxyl head groups are connected by a rigid spacer, the formation of a chelate-type complex could be more favorable. Interestingly, the isotherms had a flat collapse region at half of the monolayer areas, 43.10 and 50.52 Å^2 for Zn^{2+} and Ca^{2+}, respectively. These observations suggested the formation of bilayers which were stable enough to sustain compression.

Intricate analysis of the monolayer phase transitions was carried out from the isothermal compressibility plots. The compressibility in two dimensions is defined as $K = [-1/A\ (dA/d\pi)]$ where dA and $d\pi$ are changes in the specific area and surface pressure, respectively, of a Langmuir monolayer at the air−water interface.[33] More conveniently, the reciprocal of the compressibility (K^{-1}), termed as the static elastic modulus, is plotted. The higher the K^{-1} value, the lower is the interfacial elasticity.

Plots of the isothermal elastic modulus of racemic BDSA on subphases containing Zn^{2+} and Ca^{2+} are shown in Figure 4. When a homochiral interaction prevails, the molecules at the interface are separated into enantiomeric territories. This warrants that for a homochiral interaction, the miscibility of enantiomers tends toward minimal, resulting in enantiomerically pure domains, which otherwise would result in a racemic monolayer. Langmuir monolayers with homochiral interaction at the air−water interface will therefore resist compression because of the chiral mismatch between the domains, manifested in lower elasticity (higher K^{-1} value) of the film. The isothermal compressibility plots revealed the Zn^{2+} system to evince lower elasticity at the air−water interface when compared to that of Ca^{2+}. This suggests that the presence of Zn^{2+} ions favors a homochiral interaction at the air−water interface. Also, the observed area per molecule (90.10 Å^2) and the enhanced surface pressure corroborated the formation of monolayers with low compressibility and high rigidity.

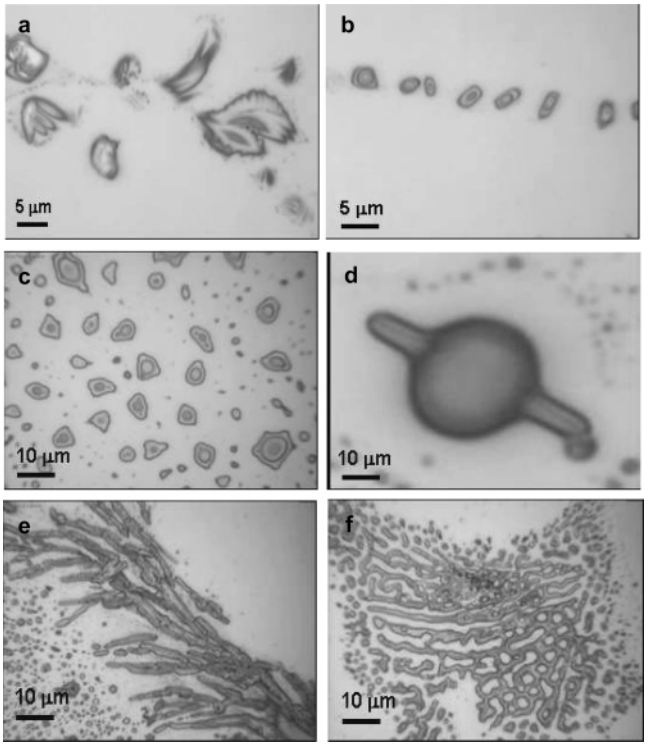

Figure 5. Optical micrographs of LB films of racemic BDSA transferred at 25 mN/ m. (a) & (b) on water subphase (c) & (d) on subphase containing 1 mM $ZnCl_2$. Micrographs (e) & (f) represent the films transferred at 42 mN/m from 1 mM $ZnCl_2$ subphase.

We believe these characteristics are due to the formation of a chelate-type complex, where the two-dimensional metal complex formation requires "preferred bite-sites" for the head groups toward Zn^{2+}, attributing enhanced stability to the film. Surface potential measurements[34] and GIXRD studies[35] have established that Ca^{2+} ions form an ionic-type complex at the interface with the fatty acid monolayers. A radially symmetric coulomb-type interaction of Ca^{2+} with the carboxyl head groups was proposed to be the phenomenon, corroborated by the low electronegativity of Ca^{2+} ions.[36]

Microscopy of the Racemic LB Films. The monolayers formed at the air−water interface were transferred onto hydrophilic quartz substrates at 25 and 45 mN/m and were examined through optical, electron, and surface force microscopic techniques. The optical images of the racemic multilayers are shown in Figure 5. The images revealed varied shapes, such as crank wheels, planetary shapes, and rings resembling vesicular structures.

The TEM images of the monolayers transferred onto carbon-coated copper grids are shown in Figure 6, evidencing corrugated sheets, wormlike aggregates, and shells formed at the air−water interface. Chiral symmetry breaking occurs when there exist thermodynamically conducive driving forces to form micelles, vesicles, or higher-order aggregates. An enantiomerically pure monolayer will have the molecules packed with zero tilt angle with respect to its nearest neighbor[37] and will show enhanced stability because of a chiral bilayer effect.[38] Chirality-dependent interactions are manifested in the condensed-phase region of the monolayers where the molecules are in close-packed configuration. Therefore, the packing is governed by the chiral identity of the neighboring molecule. This suggests that in the same monolayer, when transferred at different phases, the order of the arrangement will be differing by the different

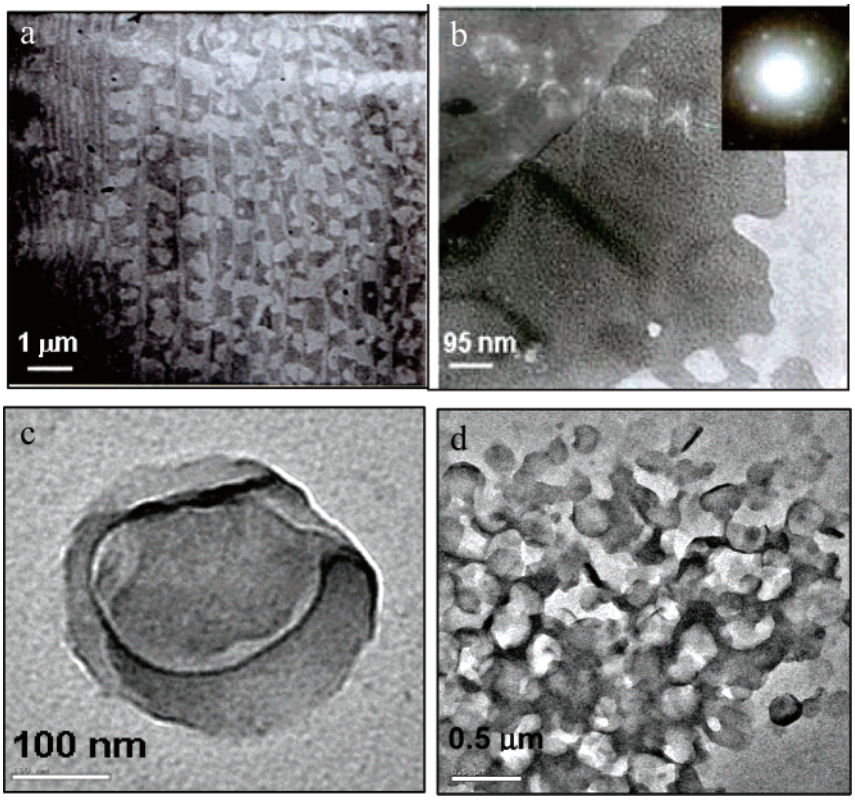

Figure 6. TEM images of LB films of racemic BDSA transferred at 25 mN/m showing (a) corrugated sheets, and (b) wormlike aggregates. Inset in (b) shows the SAED pattern evidencing the hexagonal lattice (c) shells and (d) vesicular aggregates formed at the air−water interface.

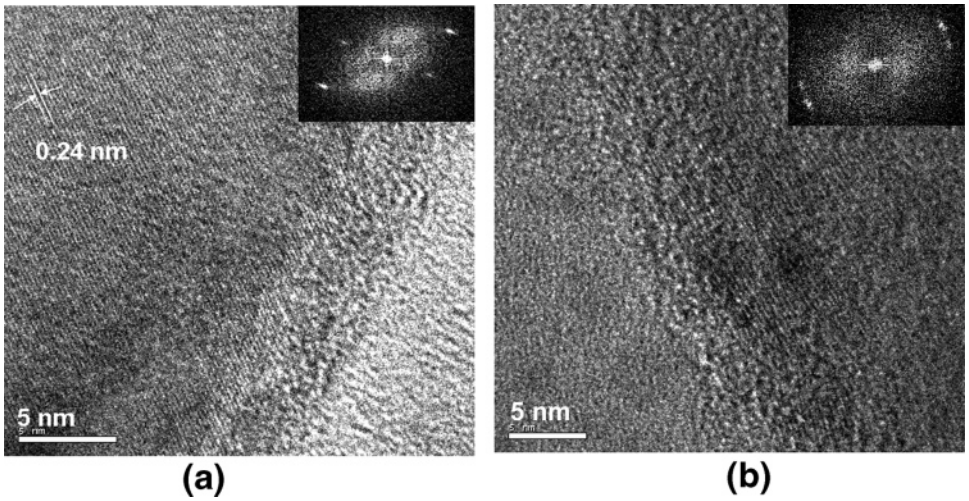

Figure 7. HRTEM images of LB films of racemic BDSA transferred at 25 mN/m from a subphase containing (a) 1 mM $ZnCl_2$ and (b) 1 mM $CaCl_2$ showing periodic lattices. The insets show the respective FFT pattern of the lattices.

scales, but the primary interactions remaining identical. The HRTEM images of the monolayers transferred at 25 mN/m from subphases containing Zn^{2+} and Ca^{2+} are shown in Figure 7. The micrographs revealed a periodicity of 0.24 nm. The FFT pattern of the Zn^{2+} lattice suggests an oblique or antipodal unit cell. Such an arrangement is possible when the unit cell possesses enantiomerically pure molecules.[39,40] The Ca^{2+} system showed a rectangular FFT pattern indicative of a heterochiral interaction.

Origin of Chiral Discrimination. Theories in continuum model parlance have been invoked to address the problem of structure or pattern formation in amphiphilic systems with a previous assumption of intrinsic chiral bending of the monolayers or the bilayers[41−44] and have employed coarse-grained Ginzburg−Landau free energy functions. A position- and orientation-dependent director embodied the molecular system with considerations toward long-range interactions. However, the molecular level interactions could be deciphered only when the interactions at the chiral centers were given explicit importance.

Andelman developed a tripodal model to explain the chiral discrimination in Langmuir monolayers[45] where the chiral center was conceived as a tetrahedron with four different groups attached. The hydrophobic tail oriented away from the water surface in the air region while the other three groups projected a tripod at the interface. The Boltzman weighted averaging of

SCHEME 1: (A) Schematic Representation of EPP Model;[a,b] (B) Schematic Structure of BDSA Molecule;[c] (C) Geometry-Optimized Structures of Zn-BDSA (B3LYP/LANL2DZ) and Ca^{2+} BDSA (B3LYP/6-31G)

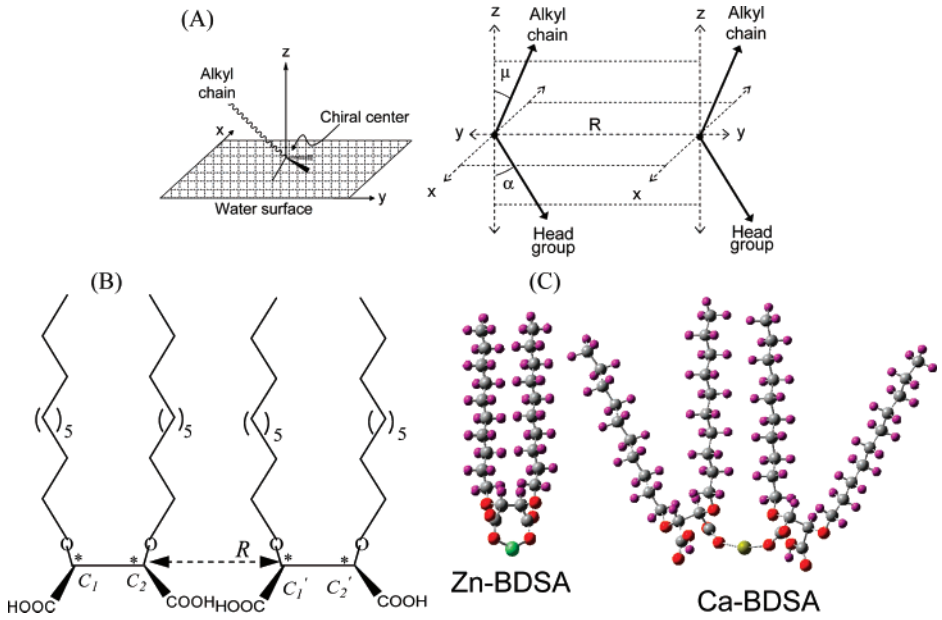

[a] Ref 48. [b] (x,y) is a plane parallel to the air−water interface, and Z is the surface normal. μ is the orientation of the alkyl chain with respect to the surface normal, and R represents the orientation of the head group. R is the intermolecular distance. [c] The chiral carbons are denoted by the asterisks and labeled as C_1, C'_1 and C_2, C'_2. The interaction between C_2 and C'_1 is isotropic in Zn^{2+}, while it is anisotropic with ionic binding with Ca^{2+}.

the van der Waals interactions predicted a heterochiral interaction, while the electrostatic interactions favored a homochiral interaction. The model was successful in predicting the chiral discrimination of systems with a single chiral center; however, it was restricted in execution, demanding a prior knowledge of the orientation of the other three substituents on the water surface. Also, the presence of a second or more chiral centers was not considered.

A closer explanation at the molecular level was developed in recent times considering the effective pair potential (EPP) between the enantiomers.[46] The driving force for the discrimination was attributed to the stereogenicity of the chiral center to result in the chiral domains of the respective handedness. The EPP approach considers the stereochemical aspects of the neighboring molecules in an assemblage of chiral molecules. The sense of the aggregate was described with effective chiral interactions explicitly retained and averaging the rest of nonchiral interactions.[47]

A minimal energy configuration of the assembly therefore is achieved by varying the distance and orientations of the substituents around the chiral center, with respect to its neighbors. In an organized assembly of amphiphiles, in its highly packed state, the twist between any two neighboring molecules decides the whole twist of the aggregate. The periodicity of the assembly is initiated by the relative twist of the neighboring molecules, with the effect propagating along the long axis with a favored twist.

Schematically, the BDSA molecule could be depicted[48] as shown in Scheme 1. The chiral carbons are marked as C_1, $C_{1'}$, and C_2, $C_{2'}$ (for one type of enantiomer). Since BDSA is a twin chiral molecule, the adjacent chiral center is actually one of the substituents attached to C_1. In such a case, the distance "R" is actually the rigid C−C bond connecting the chiral centers in BDSA. Therefore, the distance between C_1 and its immediate neighbor C_2 is fixed. The orientation of substituents around C_1 in actuality is influenced by the substituents around C_2 and, hence when a second molecule approaches, the distance "R" comes into effect. In such an arrangement, the relative orientations of the neighboring molecules are determined by the chiral identity as well as by the short-range interaction between the groups attached to the chiral centers.

The twist between any two pairs of molecules is the combination of two tilt angles in the two perpendicular planes as shown in Scheme 1A. The minimal energy configuration could be obtained when a search is performed on the whole space in which the substituents around the chiral centers are configured. The intermolecular potential between any pair of enantiomers, given in terms of a Lennard-Jones interaction of the groups, was observed to vary linearly with respect to the size of the groups attached to the chiral center.[49] Nandi et al. found that the pair potential of an $R-R$ or $S-S$ pair revealed a double minima[46] and the global minimum was found at a shorter distance of the enantiomeric pair with a definite twist angle. This is a corollary that chiral interactions are manifested in a close-packed state.

The geometry-optimized structures of Zn-BDSA and Ca-BDSA are shown in Scheme 1C. It is evident that the BDSA with a chelate-type binding to Zn^{2+} forms a more condensed monolayer than Ca^{2+} with ionic-type interaction. The above observation well matches with the experimentally observed higher area per molecule of 108.69 Å^2 for Ca^{2+}.

In the case of the Zn^{2+} salt of BDSA, the formation of the chelate-type complex "fixes" the orientation of the substituents around C_1 and C_2 (or C'_1 and C'_2). From the experimental observations of enhanced area per molecule and surface pressure, we believe that the system tries to adopt a minimal energy configuration by a homochiral interaction, where the orientations of the substituents are energetically favorable. In the presence of Ca^{2+} ions, one of the head groups is "free" to adopt its own degrees of freedom, even though its orientation is restrained by the surrounding water molecules of the subphase. The pairwise interaction ($C_2-C'_1$) is therefore anisotropic, and hence

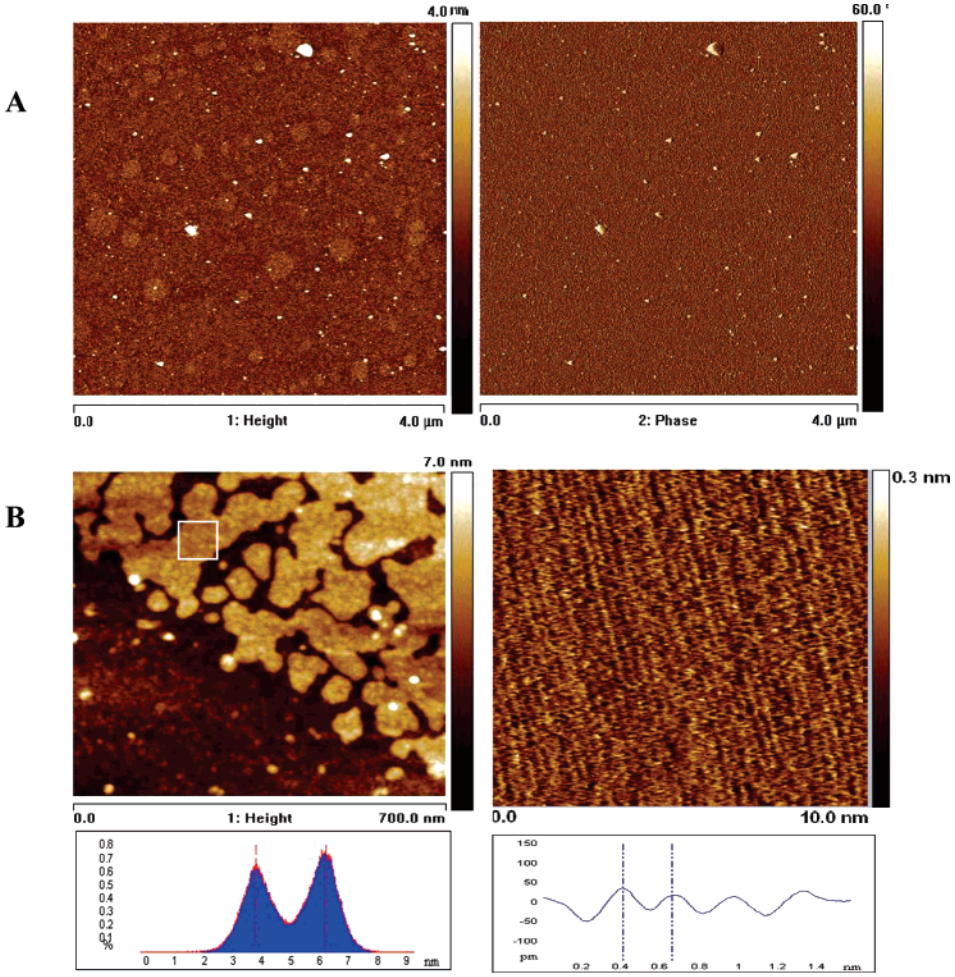

Figure 8. AFM images of (A) height and phase profiles of racemic BDSA from pure water subphase showing a uniform monolayer at 25 mN/m on Si(100). (B) racemic BDSA from a subphase containing 1 mM $ZnCl_2$ with the corresponding height profiles. A thickness of ~3 nm suggests formation of a bilayer. The image to the right evidences a repeated periodicity of 0.24 nm substrates

SCHEME 2: Centrosymmetric Arrangement of BDSA Molecules in a Bilayer[a]

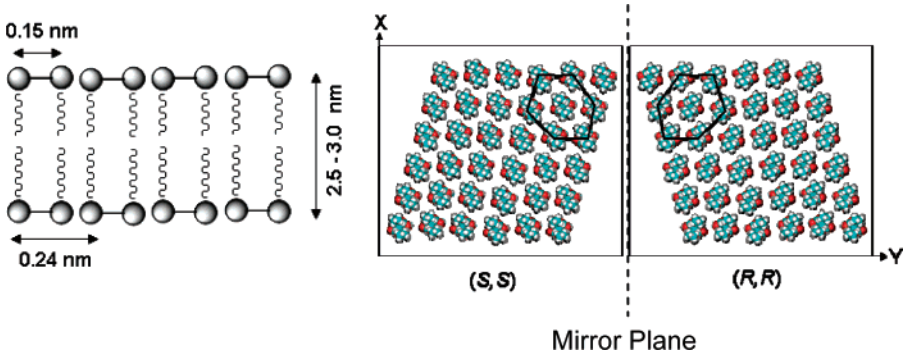

[a] The schematic to the right shows the enantiomeric homochiral domain with a hexagonal arrangement of BDSA molecules. The domains are related as object−mirror images. (x,y) represents the monolayer plane, while z is the axis of view, perpendicular to the monolayer plane.

there is an orientational mismatch of the substituents around the chiral centers, for a given pair of BDSA molecules. This induces the Ca^{2+} system to search for an orientational match of the substituents with its neighbor. The observed area per molecule of 108 Å^2 and the comparatively lower surface pressure exhibited with respect to the Zn^{2+} system suggest that Ca^{2+} prefers a heterochiral discrimination as the energetically minimal structure.

The AFM images of the monolayers transferred at 25 mN/m onto hydrophilic Si(100) substrates are shown in Figure 8. The images show highly ordered arrangements of molecules in the monolayer with a thickness of ~2.5 nm and a repeated spacing of 0.24 nm, tallying with the HRTEM analysis. The 2.5−3.0 nm height of the monolayers suggests the formation of non-interdigitated bilayers on Si(100).

Reorganization of monolayers from the as-deposited structure to a thermodynamically stable equilibrium structure has been observed in cadmium arachidate monolayers.[50,51] It has been reported that LB films of metal salts of fatty acids prefer to have a centrosymmetric bilayer as their equilibrium structure.[52]

The asymmetry prevailing in the monolayers at the air−water interface, with the alkyl chains in the air part and Zn^{2+} or Ca^{2+} in the subphase, acts as the driving force to form a centrosymmetric bilayer. In a fully extended all-trans conformation of the alkyl chain, the periodic spacing of 0.24 nm corresponds to the distance between an alkyl chain and its next-nearest neighbor.[53]

The molecule BDSA being a twin-tailed system with a rigid spacer, the next-nearest neighbor is the adjacent molecule in a state of close packing. The selected area diffraction pattern of the BDSA monolayers revealed a hexagonal arrangement in the condensed phase, which could be schematically shown as in Scheme 2. Therefore, the observed bilayer formation on the LB films could be formed of either an overturning or a creeping of the monolayers[54,55] during the transfer process. Since the bilayer orientation is maintained in the LB films, the latter mechanism would account for its formation.

Conclusions

The monolayer behavior of a new gemini-type, twin-chiral, twin-tailed molecule (2,3)-bis(decyloxy)succinic acid at the air−water interface has been explored. The system exhibited a homochiral interaction at the air−water interface. Seeding induced global ordering of the monolayers to enantiomerically pure domains was observed with 20% enantiomeric excess. The presence of metal ions in the subphase magnified the chiral interaction through 2D metal complex formation with Zn^{2+} forming a chelate-type complex and Ca^{2+} forming an ionic-type complex. AFM, TEM, and HRTEM analyses of the LB films revealed transfer-induced bilayer formation through creeping of the monolayers at the air−water interface. Effective pair potential between the enantiomers in the framework of the EPP model described the homochiral interaction in the Zn^{2+}-complexed BDSA monolayers.

Acknowledgment. The authors thank Forevision Instruments, India, and Dr. Thomas Muller, Veeco Laboratories, USA, for providing the AFM facility. B.V.S. acknowledges the research fellowship from IIT Madras.

References and Notes

(1) Nandi, N.; Vollhardt, D. *J. Phys. Chem. B* **2004**, *108*, 327.
(2) (a) Barlow, S. M.; Raval, R. *Surf. Sci. Rep.* **2003**, *50*, 201. (b) Crego-Calama, M.; Reinhoudt, D. N.; Ten-Cate, M. G. J. *Top. Curr. Chem.* **2005**, *249*, 285.
(3) Zhang, Y.; Chen, P.; Liu, M. *Langmuir* **2006**, *22*, 10246.
(4) Ajayaghosh, A.; Varghese, R.; George, S. J.; Vijayakumar, C. *Angew. Chem., Int. Ed.* **2006**, *45*, 1141.
(5) Amabilino, D. B.; Garcia, L.-P. *Chem. Soc. Rev.* **2002**, *31*, 342.
(6) (a) Stewart, M. V.; Arnett, E. M. In *Topics in Stereochemis*try; Allinger, N. L., Eliel, E. L., Wilen, S. H., Eds.; Wiley: New York, 1984. (b) Alonso, C.; Artzner, F.; Lajzerowics, J.; Grubel, G.; Boudet, N.; Rieutord, F.; Petit, J. M.; Renault, A. *Eur. Phys. J. E* **2000**, *3*, 63.
(7) Kuhnle, A.; Linderoth, R. R.; Hammer, B.; Besenbacher, F. *Nature* **2002**, *415*, 891.
(8) Martin, S. M.; Kjaer, K.; Weygand, M. J.; Weissbuch, I.; Ward, M. D. *J. Phys. Chem. B* **2006**, *110*, 14292.
(9) (a) Volkov, V. V.; Chelli, R.; Righini, R. *J. Phys. Chem. B* **2006**, *110*, 1499. (b) Overs, M.; Hoffmann, F.; Schäfer, H. J.; Hühnerfuss, H. *Langmuir* **2000**, *16*, 6995. (c) Hoffmann, F.; Hühnerfuss, H.; Stine, K. J. *Langmuir* **1998**, *14*, 4525.
(10) Vollhardt, D.; Emrich, G.; Gutberlet, T.; Fuhrhop, J.-H. *Langmuir* **1996**, *12*, 5659.
(11) Du, X.; Shi, B.; Liang, Y. *Langmuir* **1998**, *14*, 3631.
(12) Vollhardt, D.; Siegel, S.; Cadenhead, D. A. *J. Phys. Chem. B* **2004**, *108*, 17448.
(13) Kunitake, M.; Hattori, T.; Miyano, S.; Itaya, K. *Langmuir* **2005**, *21*, 9206.
(14) (a) Menger, F. M.; Littau, C. A. *J. Am. Chem. Soc*. **1991**, *113*, 1451. (b) Zana, R.; Talmon, Y. *Nature* **1993**, *362*, 228. (c) Zana, R. *Adv. Colloid Interface Sci.* **2002**, *97*, 205.
(15) Chen, X.; Wang, J.; Shen, N.; Luo, Y.; Li, L.; Liu, M.; Thomas, R. K. *Langmuir* **2002**, *18*, 6222.
(16) (a) Jiang, M.; Zhai, X.; Liu, M. *J. Mater. Chem.* **2007**, *17*, 193. (b) Jiang, M.; Zhai, X.; Liu, M. *Langmuir* **2005**, *21*, 11128. (c) Talham, D. R. *Chem. Rev.* **2004**, *104*, 5479. (d) Liang, Z.; Wang, C.; Huang, J. *Colloids Surf., A* **2003**, *224*, 213. (e) Menger, F. M.; Mbadugha, B. N. A. *J. Am. Chem. Soc.* **2001**, *123*, 875. (f) Menger, F. M.; Keiper, J. S.; Azov, V. *Langmuir* **2000**, *16*, 2062.
(17) Zhou, M.; Liu, H. L.; Yang, H. F.; Liu, X. L.; Zhang, Z. R.; Hu, Y. *Langmuir* **2006**, *22*, 10877.
(18) Buijnsters, P. J. J. A.; Rodriguez, C. L. G.; Willighagen, E. L.; Sommerdijk, N. A. J. M.; Kremer, A.; Camilleri, P.; Feiters, M. C.; Nolte, R. J. M.; Zwanenburg, B. *Eur. J. Org. Chem*. **2002**, 1397.
(19) Singh, A.; Lvov, Y.; Qadri, S. B. *Chem. Mater.* **1999**, *11*, 3196.
(20) Fouquey, C.; Lehn, J. M.; Levelut, A. M. *Adv. Mater*. **1990**, *2*, 254.
(21) Acharya, D. P.; Kunieda, H.; Shiba, Y.; Aratani, Ken-ichi. *J. Phys. Chem. B* **2004**, *108*, 1790.
(22) Shankar, B. V.; Patnaik, A. *Langmuir* **2007**, *23*, 3523.
(23) Shankar, B. V.; Patnaik, A. *J. Phys. Chem. B* **2007**, *111*, 9294.
(24) Dulyea, L. M.; Fyles, T. M.; Whitfield, D. M. *Can. J. Chem.* **1984**, *62*, 498.
(25) Valkova, L.; Borovkov, N.; Pisani, M.; Rustichelli, F. *Langmuir* **2001**, *17*, 3639.
(26) Arnett, E. M.; Thompson, O. *J. Am. Chem. Soc.* **1981**, *103*, 968.
(27) Pashley, M. R.; Karaman, M. E. *Appl. Colloid Surf. Chem.*; John Wiley: New York, 2004.
(28) Parschau, M.; Romer, S.; Ernst, K.-H. *J. Am. Chem. Soc*. **2004**, *126*, 15398.
(29) Jones, T. E.; Baddeley, C. J. *Surf. Sci*. **2002**, *519*, 237.
(30) Neumann, V.; Gericke, A.; Huehnerfuss, H. *Langmuir* **1995**, *11*, 2206.
(31) Gericke, A.; Huehnerfuss, H. *Thin Solid Films* **1994**, *245*, 74.
(32) Sakai, H.; Umemura, J. *Colloid Polym. Sci.* **2002**, *280*, 316.
(33) Hidalgo, A. A.; Pimentel, A. S.; Tabak, M.; Oliveira O. N., Jr. *J. Phys. Chem. B* **2006**, *110*, 19637.
(34) Yazdanian, M.; Yu, H.; Zografi, G. *Langmuir* **1990**, *6*, 1093.
(35) Datta, A.; Kmetko, J.; Richter, A. G.; Yu, C.-J.; Dutta, P.; Chung, K.-S.; Bai, J.-M. *Langmuir* **2000**, *16*, 1239.
(36) Datta, A.; Kmetko, J.; Yu, C.-J.; Richter, A. G.; Chung, K.-S.; Bai, J.-M.; Dutta, P. *J. Phys. Chem. B* **2000**, *104*, 5797.
(37) Shimizu, T.; Masuda, M.; Minamikawa, H. *Chem. Rev.* **2005**, *105*, 1401.
(38) Furhop, J. H.; Schnieder, P.; Rosenberg, J.; Boekema, E. *J. Am. Chem. Soc.* **1987**, *109*, 3387.
(39) Zhang, Y. J.; Song, Y.; Zhao, Y.; Li, T. J.; Zhu, D. *Langmuir* **2001**, *17*, 1317.
(40) Eckhardt, C. J.; Peachey, N. M.; Swanson, D. R.; Takacs, J. M.; Khan, M. A.; Gong, X.; Kim, J.-H.; Wang, J.; Uphaus, R. A. *Nature* **1993**, *362*, 614.
(41) Helfrich, W.; Prost, J. *Phys. Rev. A* **1988**, *38*, 3065.
(42) Lubensky, T. C.; Prost, J. *J. Phys. II* **1992**, *2*, 371.
(43) Zhong-Can, O.; Ji-Xing, L. *Phys. Rev. A* **1993**, *71*, 4091.
(44) Selinger, J. V.; Spector, M. S.; Schnur, J. M. *J. Phys. Chem. B* **2001**, *105*, 7157.
(45) (a) Andelman, D. *J. Am. Chem. Soc*. **1989**, *111*, 6536. (b) Andelman, D.; Orland, H. *J. Am. Chem. Soc.* **1993**, *115*, 12322.
(46) Nandi, N.; Bagchi, B. *J. Am. Chem. Soc.* **1996**, *118*, 11208.
(47) Nandi, N.; Bagchi, B. *J. Phys. Chem. A* **1997**, *101*, 1343.
(48) Nandi, N.; Vollhardt, D. *Chem. Rev.* **2003**, *103*, 4033.
(49) Ben-Amotz, D.; Herschbach, D. R. *J. Phys. Chem.* **1990**, *94*, 1038.
(50) Holden, M. A.; Jung, S.-Y.; Yang, T.; Castellana, E. T.; Cremer, P. S. *J. Am. Chem. Soc.* **2004**, *126*, 6512.
(51) Takamoto, D. Y.; Aydil, E.; Zasadsinski, J. A.; Ivanova, A. T.; Schwartz, D. K.; Yang, T.; Cremer, P. S. *Science* **2001**, *293*, 1292.
(52) Corkery, R. W. *Langmuir* **1997**, *13*, 3591.
(53) Hibino, M.; Sumi, A.; Tsuchiya, H.; Hatta, I. *J. Phys. Chem. B* **1998**, *102*, 4544.
(54) Schwartz, D. K.; Viswanathan, R.; Zasadzinski, J. A. N. *J. Phys. Chem.* **1992**, *96*, 10444.
(55) Wiesler, D. G.; Feigin, L. A.; Majkrzak, C. F.; Ankner, J. F.; Berzina, T. S.; Troitsky, V. I. *Thin Solid Films* **1995**, *266*, 69.